Synthesis of size tunable monodispersed silver nanoparticles and the effect of size on SERS enhancement

Richard N. Cassar, Duncan Graham, Iain Larmour, Alastair W. Wark, and Karen Faulds
Pure and Applied Chemistry, University of Strathclyde,
295 Cathedral Street, Glasgow,
G1 1XL,
UK
E-mail: Duncan.Graham@strath.ac.uk
Keywords: hydroquinone reduction; silver nanoparticle synthesis; surface-enhanced Raman scattering

Abstract

Spherical and monodispersed silver nanoparticles (AgNPs) are ideal for fundamental research as the contribution from size and shape can be accounted for in the experimental design. In this paper a seeded growth method is presented, whereby varying the concentration of sodium borohydride reduced silver nanoparticle seeds different sizes of stable spherical nanoparticles with a low polydispersity nanoparticles are produced using hydroquinone as a selective reducing agent. The surface-enhanced Raman scattering (SERS) enhancement factor for each nanoparticle size produced (17, 26, 50, & 65 nm) was then assessed using three different analytes, rhodamine 6G (R6G), malachite green oxalate (MGO) and thiophenol (TP). The enhancement factor gives an indication of the Raman enhancement effect by the nanoparticle. Using non-aggregated conditions and two different laser excitation wavelength (633 nm and 785 nm) it is shown that an increase in particle size results in an increased enhancement for each analyte used.

1. Introduction

Inorganic nanoparticles are being used in an increasing amount of applications due to their properties such as photoluminescence (e.g. CdSe and CdTe), magnetic moment

(e.g. iron oxide and cobalt), particle plasmon resonance absorption (e.g. silver and gold)[1, 2]. The latter are finding huge potential in applications for sensitive optical diagnostic tools due to the high electron and strong optical absorption, which makes them ideal candidates as substrates for SERS. This spectroscopic method, the Raman signal of an analyte which is intrinsically weak can be enhanced when absorbed or in close proximity to a silver or gold nanoparticle surface. AgNPs were used in the first claims of single molecule detection both in colloid solutions[3] and on a planar substrate[4].

Since the particle plasmon resonance absorption is dependent on various factors such as the surface, the dielectric constant of the metal, the shape and the size of the particle, it is important to have a well-characterized substrate. This gives the rise to the need of nanoparticle synthesis that produce reproducible, homogenous and monodispersed nanoparticles. There are various synthesis routes by which silver and gold nanoparticles[5] are obtained. While the preparation of spherical monodispersed gold nanoparticles are well characterized the preparation of AgNPs still seems to pose a challenge to produce spherical monodispersed nanoparticles which are suitable as SERS substrates. Most of these preparations result in polydispersed sols with different morphologies[6-8]. Other methods for preparing different sized monodispersed AgNPs using conventional polyol method[9], however the poly(vinyl pyrrolidone) coats the nanoparticle making it difficult for the surface to be accessible to the analyte to be detected by SERS.

This paper therefore tackles this challenge and expands on previous hydroquinone (HQ)[10, 11] reduction methods. A simple and effective method for the preparation of a wide range of sizes of spherical monodispersed nanoparticles using a seeded growth method is shown. A desired size of nanoparticle can be easily obtained by changing

the seed concentration while keeping all other reagents constant. This was done by using sodium borohydride reduced silver nanoparticles as seeds and HQ as the reducing agent for the $AgNO_3$ salt. HQ is a selective reducing agent as it allows silver ions to be reduced only on the seed particles present and thus reduces secondary nucleation sites giving better monodispersity. The different size ranges of nanoparticles produced were subsequently tested for their efficiency as SERS substrates to find the optimal size at which the maximum intensity is delivered. Such a study is important as it is known that the enhancement increases with particle size increase[12, 13], however it follows that an increase in size also means nanoparticles absorb less and scatter more through inelastic scattering[14], this can be explained by scaling differences between absorption and scattering[15]. An increase in size of AgNPs whilst the Ag concentration remains constant implies that the surface area available for the analyte to adsorb decreases. Hence the overall effect on the SERS response is a balance between enhancement, scattering and surface area. To avoid overestimation of the SERS enhancement the enhancement factor has to be real, that is an enhancement that would not be present under non-SERS conditions for the same molecule. SERS enhancement factors are usually separated into two main multiplicative contributions; the electromagnetic (EM) enhancement and the chemical enhancement (CE). The EM enhancement is due to the coupling of the incident and Raman electromagnetic field with the SERS substrate, while the CE origins are still controversial [16]. The most widely accepted mechanism for the latter is through a charge transfer mechanism [17]. The EM enhancement factor is thought to be the dominant contribution, however it is not necessary to know the exact origin to measure the overall enhancement factor.

In fact in this paper three analytes with different optical and chemical properties are used giving the possibility of understanding better the effect of nanoparticle size on different analytes by measuring the analytical enhancement factor (AEF). Since the AEF strongly depends on the adsorption properties and surface coverage of the probe identical experimental conditions were used with all the different sizes and analytes used. AEF measurements are easily obtained and reproducible therefore can be used to monitor the average effect of nanoparticle size on the SERS signal.

2. Materials and Methods

2.1 Chemicals and Materials.

Silver nitrate ($AgNO_3$, ≥99%), hydroquinone ($C_6H_6O_2$, ≥99%), trisodium citrate dihydrate ($Na_3C_6H_5O_7 \cdot 2H_2O$, 99%), sodium borohydride ($NaBH_4$, 99%) rhodamine 6G (R6G) ($C_{28}H_{31}N_2O_3Cl$, 98%), malachite green oxalate ($C_{52}H_{54}N_4O_{12}$), thiophenol (C_6H_6S, ≥99%), ethanol (C_2H_6O, 99%). All chemicals were purchased from Sigma-Aldrich and used without further purification. All water used was doubly distilled (18.2 mΩ cm).

2.2 Synthesis of AgNPs.

The synthesis of the different sizes of AgNPs were prepared by a two step process; the preparation of AgNP seeds by sodium borohydride reduction, followed by a controlled seeded growth of the AgNP seeds with the reduction of $AgNO_3$ with hydroquinone. All glassware was soaked in *aqua regia* for two hours and thoroughly rinsed with doubly distilled water.

2.2.1 Seed preparation.

The sample preparation method used is a modification of the method reported by Creighton et al.[6]. The Ag colloid seed solution was prepared by preparing a 0.002 m

sodium citrate solution (10 mL). Under vigorous stirring to the latter solution of 0.1 m $AgNO_3$ (50 μL) was added followed by a drop wise addition of 0.1 M $NaBH_4$ (1 mL).

2.2.2 AgNPs with controlled size ranges procedure.

The sample preparation method used is a modification of the method reported by Gentry et al.[10]. The different sizes of AgNPs were prepared by varying the amount of seed concentration whilst keeping all other reagents concentration constant. Hence a 0.1 M $AgNO_3$ (100 μL) solution was added to a varying volume of H_2O (7.2 mL – 9.7 mL) in a 15 mL scintillation flask. Under rapid stirring at room temperature a varying volume of sodium borohydride reduced silver nanoparticles (0.08 mL – 2.56 mL) were added followed by 0.1 M sodium citrate (22 μL) and of 0.03 M (100 μL) hydroquinone, thus giving a final solution volume of 10 mL.

2.3 Instrumentation and Measurements:

2.3.1 UV/Vis Spectroscopy.

The extinction spectra of the colloids were recorded using a Varian Cary 300 Bio spectrophotometer directly after preparation of each nanoparticle size over a wavelength range of 200-800 nm. The extinction spectra of the colloid were recorded again after addition of the analytes. The baselines were recorded using doubly distilled water and the samples were diluted accordingly to remain in the absorption response limit of the spectrometer. The seed concentration was calculated by Beer-Lamberts' law whereby the extinction coefficient used was 4.16×10^9 M^{-1} cm^{-1}.

2.3.2 Scanning Electron Microscopy.

A sample from each nanoparticle preparation was prepared on a polycation functionalized silicon wafer. The wafer was first cleaned using water and ethanol, then dried in a nitrogen flow. The wafer was then placed in an oxygen plasma cleaner for 60 seconds. PDDA (30 μL) was dissolved in 1 mM NaCl (1 mL), the solution was

used to coat the clean wafer by spotting the wafer with the solution with a pipette and then leaving it for 30 minutes under a water-saturated atmosphere. After this step it was washed off and dried in a nitrogen flow. Each AgNP (100 μL) sample was put onto the PDDA-functionalized silicon wafer for 15 minutes under a water-saturated atmosphere. The sample was then washed off and dried in a nitrogen flow. Using a scanning electron microscope (FEI Sirion 200 ultra-high-resolution Schottky Field emission gun), eight 'snapshot' images were taken for each sample. From the images obtained the diameter was calculated using Image J[18], an image processing and analysis software. An automated method was used to measure the particles, whereby the particles must have a range between 10 nm – 100 nm and the circularity of the particles must be around 0.8 – 1 (where circularity is defined as Circularity = $4\pi(\text{Area}/\text{Perimeter}^2)$) as to avoid any aggregates that might be present. Before the particles were measured the images were converted to gray scale 8-bit images, enhanced by binary contrast enhancement (tresholding) and the scale was calibrated. More than 600 particles were measured for each size.

2.3.3 Dynamic Light Scattering (DLS) and Zeta-potential measurements.

The size and zeta-potential of the different sized AgNPs were measured before and after addition of MGO, R6G and TP using a Malvern Zetasizer (Nano-ZS) instrument. The standards for size were Nanosphere size standards 20 nm (± 1.5 nm, Lot. 339300) and 40nm (±1.8 nm, Lot. 33306), while the standard for the zeta-potential used was zeta-potential transfer standard (-68mV ± 6.8mV, Batch No. 051001).

2.3.4 Raman Measurements

To 300 μL of AgNP, 33 μL of $1.6\text{x}10^{-5}$ m R6G solution were added to give a final concentration of dye of $1.6\text{x}10^{-6}$ m. The same volumes and concentrations were used for the other analytes MGO and TP.

The SERS spectra of three identical samples was recorded after one minute of mixing the analyte with the AgNPs with an instrumental setup in a confocal arrangement at an extinction wavelength of 633 nm. The SERS spectra were obtained with an exposure time of 2 seconds and 5 accumulations. The setup consisted of a Leica DM/LM microscope equipped with an Olympus 20x/0.4 long-working distance objective that collects 180º backscattered light from a cuvette. The spectrometer system was Renishaw Ramascope System 2000 (Gloucestershire, UK). The same procedure using the same experimental setup was used using an excitation wavelength of 785 nm with an exposure of 20 seconds and 5 accumulations.
0.01M solutions of MGO andR6G, and a 9.3m TP ethanolic solution TP. A $1x10^{-6}$ m MGO solution was prepared to obtain a Raman spectrum at 633 nm laser excitation wavelength. The Raman spectra of three identical samples were recorded using the same experimental conditions and setup as described previously for obtaining the surface enhanced Raman spectra.

3. Results and Discussion

In this study a range of sizes of silver nanoparticles were prepared using an improved method, which give monodispersed spherical particles. The optimal size for SERS was then assessed by comparing the signals from the different sizes prepared to the signal from an unenhanced Raman experimental setup. Silver was chosen for the study not only because it has a strong optical response and a narrower particle plasmon resonance than gold[19-22] but also due to the need of a well characterized method for preparation of homogenous monodispersed AgNPs.

3.1 Synthesis and Characterization

The AgNPs were synthesized using HQ as a selective reducing agent using a modified version of the seeded growth method used by Gentry et al.[10]. In this paper it is shown that different sized nanoparticles can be prepared by varying the seed concentration. Other seeded growth methods have already been reported both for gold and silver nanoparticles[10, 23-26] but not with HQ as a reducing agent. HQ is widely used in photographic film development and selectively reduces silver ions in the presence of metallic silver nanoclusters[10, 27, 28]. The weak reducing potential of HQ (E^o = -0.699 v NHE) is unable to reduce isolated Ag^+ as it has a more negative reducing potential of -1.8V. However Ag^+ can be reduced in the presence of silver (Ag^0) as the reducing potential changes to +0.799 V.

For the synthesis of different sized silver nanoparticles, HQ was used as it is a weak reducing agent and as mentioned above it selectively reduces silver ions only in the presence of AgNP seeds as represented in figure 1. Reduction by HQ has its own practical aspects as the reduction reaction is complete in a short period of time (15 minutes maximum) and it occurs at room temperature. Also HQ gives poor steric hindrance but also binds weakly to the silver surface of nanoparticles therefore such nanoparticles can be easily modified with different modifiers which would be better suited for subsequent applications.

FIGURE 1

The nanoparticles prepared by HQ in this paper were stabilized with sodium citrate. The seed used for the growth of the nanoparticles were prepared by sodium borohydride reduction of silver nitrate, which give small enough nanoparticles to serve as seeds onto which further layers of silver can be added on. This nanoparticle preparation is reported to produce polydispersed sols and particles of different morphologies[6], as can be confirmed from the SEM images obtained (see figure 2a).

The nanoparticles grown from the seeds however are monodispersed and of a spherical shape as confirmed by the SEM images (see figure 2 b-e). The different sizes were produced by varying the concentration of the seed while keeping the amount of silver nitrate and HQ constant (see table 1).

TABLE 1

As the seed concentration is gradually decreased less nanoparticles will be available for the silver nitrate to be reduced on to therefore larger nanoparticles are gradually produced. It is to note that the silicon wafers were treated with PDDA a polycation which due to the positive charges on its backbone prevents aggregation of the negatively charged AgNPs during the drying process in the SEM preparation steps due to Coulombic attractions. The images obtained then give a better representation of what is in solution. As seen in figure 2 b-e very few aggregates are present, suggesting that no nanoparticle clusters are present in solution.

FIGURE 2

The four samples produced were characterized by SEM, whereby eight SEM images from each sample were measured by an automated process on Image J [18] software from which it was calculated that as the seed concentration is decreased from 0.542 to 0.009 nM the size increased from 17 nm to 65 nm (see table 1) and that the samples produced are relatively monodispersed as the SEM images in figure 2(b-e). The full width at half maximum (FWHM), as well as the standard deviation increase as the size of the AgNPs increases (see table 1).

This broadening of the extinction spectra can be attributed to additional multipolar resonances which become more significant as the particles get larger [21] and as expected a red shift was observed as the size is increased starting from a maximum of 390 nm for the seed up to 513 nm for the larger nanoparticles[12, 29-33] (figure 3).

FIGURE 3

The extinction spectra (figure S1), size (figure S2) and zeta-potential (figure S3) of the AgNPs were measured before and after addition of the analytes to check nanoparticle stability. The DLS shows different particle sizes for the different samples of AgNPs produced for which after most additions of analyte no significant shift in the nanoparticles' extinction spectra were observed and the DLS data show no significant increase in the hydrodynamic diameter. The zeta-potential for all different sized AgNPs produced show that stable particles are produced as the zeta-potential is around -30mV, due to the citrate layer that is adsorbed to the nanoparticle surface. A slight decrease in zeta-potential can be observed suggesting that the analytes has adsorbed to the surface without causing any aggregation of the colloid (figure S3). On the other hand when TP was added it is interesting to note that for the larger sized nanoparticles aggregation occurs as a red-shift is observed in the extinction spectra, aggregation was also confirmed by the DLS data and the zeta-potential measurements. (figures S1, S2, & S3).

3.2 Surface Enhanced Raman Scattering

The extinction spectra of the nanoparticles produced have a low extinction above 600 nm therefore being off-resonance with the 633 and 785 nm laser excitation used. The analytes chosen to study the effect of spherical AgNP size on SERS intensity were the dyes rhodamine 6 G (R6G) and malachite green oxalate (MGO) and the sulfur containing molecule thiophenol (TP).

The three analytes adsorb to the surface (chemisorbed for TP and physisorbed for MGO & R6G) of the negatively charged AgNPs as R6G and MGO are positively charged dyes, while TP has a thiol group which has a great affinity towards silver[34-

36]. The two dyes have been extensively studied in SERS experiments as they have reliable photostability[35, 37, 38]. R6G has a maximum adsorption of 530 nm and is off-resonance with both excitations used however MGO which has an excitation maximum at 621nm, therefore at 633 nm is in resonance with the laser. This gives the possibility to compare between off-resonance and resonance SERS intensity with different sizes. The non-dye analyte thiophenol was used which is off-resonance to both laser wavelengths used, and no fluorescence or photobleaching hinders the SERS measurement.

The Raman enhancement effect in the SERS experiment was determined by the AEF, which is denoted by *G,* describes the enhancement of the Raman signal per molecule adsorbed on the surface of a SERS-active species (in this case AgNPs)[39, 40]. *G* is calculated as:

$$\boldsymbol{G = \frac{I_{SERS}}{I_{Raman}} \frac{M_{Bulk}}{M_{Monolayer}}} \qquad \textbf{(1)}$$

where I_{SERS} and I_{Raman} are the Raman intensity enhanced by AgNPs and unenhanced intensity respectively. M_{Bulk} and $M_{Monolayer}$ are the molar concentrations of the analyte in an unenhanced experiment and enhanced experiment respectively. $M_{Monolayer}$ for the different sizes of AgNPs produced was calculated (see supplementary information) assuming total nanoparticle surface coverage of the analytes, whereby a single R6G molecule occupies an area of 0.4 nm^2 on the surface of the AgNP[41]. This value was used as an approximate value for MGO. While for TP a single molecule occupies and area of 0.3 nm^2 [36]. To ensure monolayer coverage around the nanoparticles a concentration of 1.6×10^{-6} M of analyte was used (see figure S4 in the supporting information). The Raman spectra for all three analytes from which I_{Raman} were obtained at a higher analyte concentration than in the SERS condition experiments, as peaks could not be resolved at those low concentrations. The Raman spectrum of

MGO at 633 nm excitation wavelength however had to be taken at a concentration of 1μM due to the high fluorescence background as the laser excitation wavelength was close to the absorption peak of the dye.

The SERS intensity for the different AgNPs sizes were monitored at two different Raman peaks for each analyte used (see figure S5 in the supporting information). The Raman shift of 1361 cm^{-1} (in-plane bending and aromatic C-C stretching) and 1508 cm^{-1} (aromatic C-C stretching) for R6G were used, while for MGO 1365 cm^{-1} (N-C stretch) and 1395 cm^{-1} (C-C and C-H in-plane motion aromatic) and for TP 997 cm^{-1} (in-plane ring breathing mode) and 1022 cm^{-1} (in-plane C-H bend) were used[42, 43]. These bands were chosen as no shift in frequency is observed when going from the Raman spectrum of the neat analyte solution to the spectrum taken under SERS conditions, that is the frequency of the vibration chosen are not effected by the adsorption to the surface of the nanoparticle (see figure 4).

FIGURE 4

It is to note however that the SERS spectrum of TP has a few changes when compared to neat TP. These changes are due to the adsorption of the molecule to the silver surface[43, 44]. The band at 917cm^{-1} in the Raman spectrum which is attributed to the bending vibration of the S-H bond is no longer detected which indicates that the TP is chemisorbed on silver surface by the breaking of the S-H bond. Further evidence of TP is S-bonded to the metal surface is the shift of the 1092cm^{-1} peak (ring-breathing mode coupled to the ν(C-S) mode) further down to 1068cm^{-1} [44](see figure 4)

3.3 SERS vs. Size

For the samples where no aggregation occurred after addition of the analyte as expected[39], the SERS intensity and the *G* value increases with particle diameter as

electromagnetic enhancement increases with size (see table 2) . For TP addition an increase in intensity and *G* value was also observed however contribution by aggregation for the larger sized nanoparticles affected the SERS intensity.

TABLE 2

Nonetheless the fact that an increase in enhancement factor was observed for all three different analytes suggests that SERS intensity is not only probe dependent.

MGO which absorbs at 621 nm is close to the 633 nm laser wavelength used and an enhancement can be seen for all nanoparticle sizes. On going to a longer laser wavelength (785 nm) spectra can be still be obtained for most nanoparticle sizes, with enhancement increasing with size. It is to note that the enhancement at 785 nm is greater than at 633 nm laser excitation, this can be due to the dye being resonant at 633 nm and some degree of photobleaching of the dye occurs which in turn reduces the SERS intensity. When using R6G however which is off-resonance with both laser wavelengths used enhancement of the Raman spectra at the concentration used in the experiment can only be seen for larger sized nanoparticles, this can be attributed to a reduced adsorption efficiency of the dye molecule due to the lack of colloid activation by NaCl as suggested by Kneipp et al.[45]. A higher enhancement factor is given at 633 nm laser excitation wavelength close to R6G absorption maximum though still being off-resonance rather than at a longer 785 nm wavelength.

For TP (a good Raman scatterer molecule) SERS spectra were obtained for all of the peaks monitored, even for the small sized nanoparticles where no aggregation occurred upon addition of TP. Enhancement factors are high even for smaller sizes of AgNPs when TP is used. This can be due to the adsorption of the molecule through the formation of a thiol bond between the silver and sulfur. If it is assumed that the benzene ring of TP extends out of the AgNP surface, the Raman modes which are

aligned with the local field are favored hence a larger enhancement factor for the peaks observed, even at small silver nanoparticle size. For the larger nanoparticles aggregation played an important role in enhancement of the Raman peaks hence the enhancement cannot be solely related to the size of the nanoparticles.

This study shows us that for non-aggregated SERS experiments larger AgNPs are ideal for both on- and off-resonance setups, whereby the larger SERS intensities and enhancements are given.

4. Conclusion

A simple and fast method for the production of spherical, monodispersed nanoparticles of tunable size by the selective reduction of $AgNO_3$ on silver seeds with HQ is reported. It was concluded that the maximum enhancement of the Raman spectrum and SERS intensities for all three analytes MGO, R6G, and TP in SERS conditions is with 65 nm AgNPs. These particles have the potential for being used for other diagnostic purposes in off-resonance and in-resonance setups, as their optical response can be modified by simple tuning of their size.

Acknowledgements

The authors would like to thank the Strategic Educational Pathways Scholarship (STEPS, Malta) and the European Social Fund (ESF) for the scholarship award to R.N.C.

Supporting Information

Supporting information maybe be found in the online version of this article.

References

[1] V. Biju, T. Itoh, A. Anas, A. Sujith, M. Ishikawa, Analytical and Bioanalytical Chemistry, 391 (2008) 2469-2495.
[2] R.A. Sperling, W.J. Parak, Philosophical Transactions of the Royal Society A: Mathematical, Physical and Engineering Sciences, 368 (2010) 1333-1383.
[3] K. Kneipp, Y. Wang, H. Kneipp, L.T. Perelman, I. Itzkan, R.R. Dasari, M.S. Feld, Phys. Rev. Lett., 78 (1997) 1667.
[4] S. Nie, S.R. Emory, Science, 275 (1997) 1102-1106.
[5] O. Masala, R. Seshadri, Ann. Rev. Mater. Res., 34 (2004) 41-81.
[6] J.A. Creighton, C.G. Blatchford, M.G. Albrecht, J. Chem. Soc., Faraday Trans. 2, 75 (1979) 790-798.
[7] P.C. Lee, D. Meisel, J. Phys. Chem., 86 (1982) 3391-3395.
[8] D.L. Van Hyning, C.F. Zukoski, Langmuir, 14 (1998) 7034-7046.
[9] H. Li, L.J. Rothberg, J. Am. Chem. Soc., 126 (2004) 10958-10961.
[10] S.T. Gentry, S.J. Fredericks, R. Krchnavek, Langmuir, 25 (2009) 2613-2621.
[11] M.A. Perez, R. Moiraghi, E.A. Coronado, V.A. Macagno, Crystal Growth & Design, 8 (2008) 1377-1383.
[12] K.L. Kelly, E. Coronado, L.L. Zhao, G.C. Schatz, J. Phys. Chem. B, 107 (2003) 668-677.
[13] V.N. Pustovit, T.V. Shahbazyan, Microelectron. J., 36 (2005) 559-563.
[14] E.C. Le Ru, P.G. Etchegoin, Principles of Surface-Enhanced Raman Spectroscopy, Elsevier, Amsterdam, 2009.
[15] S.A. Maier, Plasmonics: Fundamentals and Applocations, Springer, New York, 2007.
[16] R. Aroca, Surface-Enhanced Infrared Spectroscopy, in: Surface-Enhanced Vibrational Spectroscopy, John Wiley & Sons, Ltd, 2007, pp. 185-222.
[17] J.R. Lombardi, R.L. Birke, T. Lu, J. Xu, The Journal of Chemical Physics, 84 (1986) 4174-4180.
[18] M.D. Abramoff, P.J. Magelhaes, S.J. Ram, Biophotonics International, 11 (2004) 36-42.
[19] C.F. Bohren, D.R. Huffman, Absorption and scattering of light by small particles, Wiley, New York 1998.
[20] H. Xu, J. Aizpurua, M. Kall, P. Apell, Phys. Rev. E, 62 (2000) 4318.
[21] J. Yguerabide, E.E. Yguerabide, Anal. Biochem., 262 (1998) 137-156.
[22] J. Yguerabide, E.E. Yguerabide, Anal. Biochem., 262 (1998) 157-176.
[23] L. Cao, T. Zhu, Z. Liu, J. Colloid Interface Sci., 293 (2006) 69-76.
[24] N.R. Jana, L. Gearheart, C.J. Murphy, Adv. Mater., 13 (2001) 1389-1393.
[25] N.R. Jana, L. Gearheart, C.J. Murphy, The Journal of Physical Chemistry B, 105 (2001) 4065-4067.
[26] H. Yu, P.C. Gibbons, K.F. Kelton, W.E. Buhro, J. Am. Chem. Soc., 123 (2001) 9198-9199.
[27] T. Linnert, P. Mulvaney, A. Henglein, H. Weller, J. Am. Chem. Soc., 112 (1990) 4657-4664.
[28] M. Mostafavi, J.L. Marignier, J. Amblard, J. Belloni, International Journal of Radiation Applications and Instrumentation. Part C. Radiation Physics and Chemistry, 34 (1989) 605-617.
[29] P. Lundahl, R. Stokes, E. Smith, R. Martin, D. Graham, Micro & Nano Letters, IET, 3 (2008) 62-65.

[30] I. Pastoriza-Santos, L.M. Liz-Marzan, J. Mater. Chem., 18 (2008) 1724-1737.
[31] O. Siiman, L.A. Bumm, R. Callaghan, C.G. Blatchford, M. Kerker, The Journal of Physical Chemistry, 87 (1983) 1014-1023.
[32] C.S. Seney, B.M. Gutzman, R.H. Goddard, The Journal of Physical Chemistry C, 113 (2008) 74-80.
[33] K.G. Stamplecoskie, J.C. Scaiano, J. Am. Chem. Soc., 132 (2010) 1825-1827.
[34] C.H. Munro, W.E. Smith, M. Garner, J. Clarkson, P.C. White, Langmuir, 11 (1995) 3712-3720.
[35] X. Qian, S.R. Emory, S. Nie, J. Am. Chem. Soc., 134 (2012) 2000-2003.
[36] J.Y. Gui, D.A. Stern, D.G. Frank, F. Lu, D.C. Zapien, A.T. Hubbard, Langmuir, 7 (1991) 955-963.
[37] J. Wrzesien, D. Graham, Tetrahedron, 68 (2012) 1230-1240.
[38] V.S. Tiwari, T. Oleg, G.K. Darbha, W. Hardy, J.P. Singh, P.C. Ray, Chem. Phys. Lett., 446 (2007) 77-82.
[39] K.G. Stamplecoskie, J.C. Scaiano, V.S. Tiwari, H. Anis, The Journal of Physical Chemistry C, 115 (2011) 1403-1409.
[40] E.C. Le Ru, E. Blackie, M. Meyer, P.G. Etchegoin, J. Phys. Chem. C, 111 (2007) 13794-13803.
[41] R. Sasai, T. Fujita, N. Iyi, H. Itoh, K. Takagi, Langmuir, 18 (2002) 6578-6583.
[42] A.C. Power, A.J. Betts, J.F. Cassidy, Analyst, 136 (2011) 2794-2801.
[43] M.A. Bryant, S.L. Joa, J.E. Pemberton, Langmuir, 8 (1992) 753-756.
[44] T.H. Joo, M.S. Kim, K. Kim, J. Raman Spectrosc., 18 (1987) 57-60.
[45] K. Kneipp, Y. Wang, R.R. Dasari, M.S. Feld, Appl. Spectrosc., 49 (1995) 780-784.

Figures

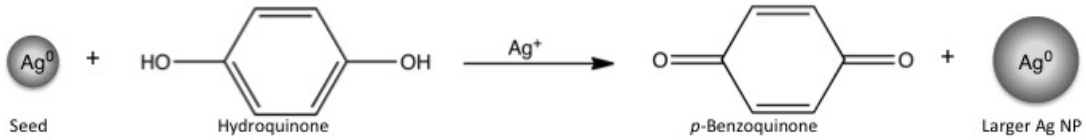

Figure 1. Schematic representation of growth of silver seeds (left) into larger silver nanoparticles by the reduction of silver ions by hydroquinone.

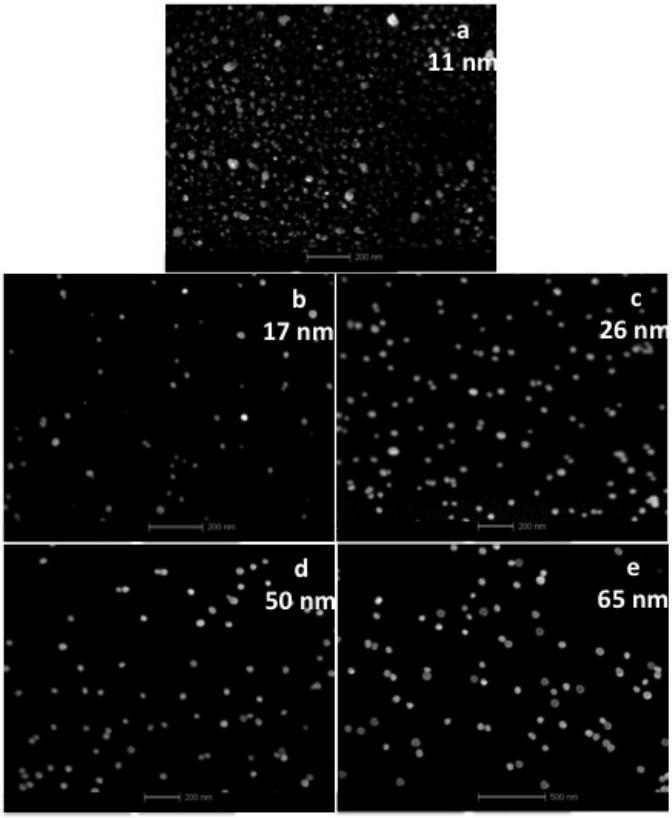

Figure 2. Sample SEM images of seed (a) and AgNPs (b-e) produced by the seed growth method. Images a to e correspond to average sizes of 11, 17, 26, 50, and 65 nm, respectively. Note that scale bars in images a-d are 200 nm while for image e the scale bar is 500 nm.

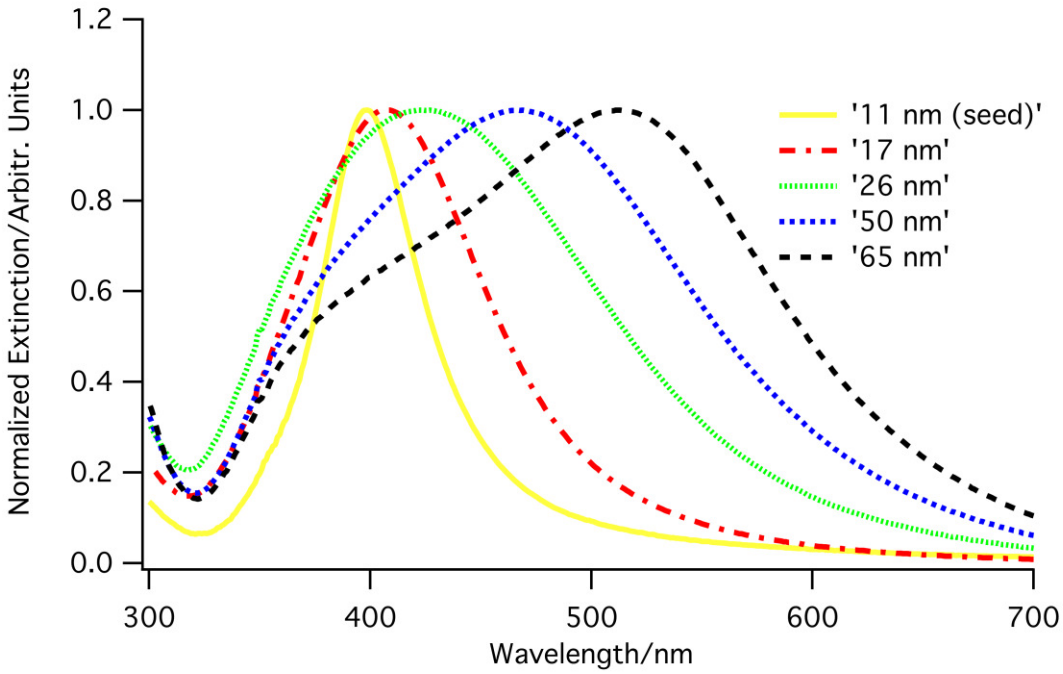

Figure 3. Normalized extinction spectra of seed and seed growth nanoparticles corresponding to SEM images in figure 2.

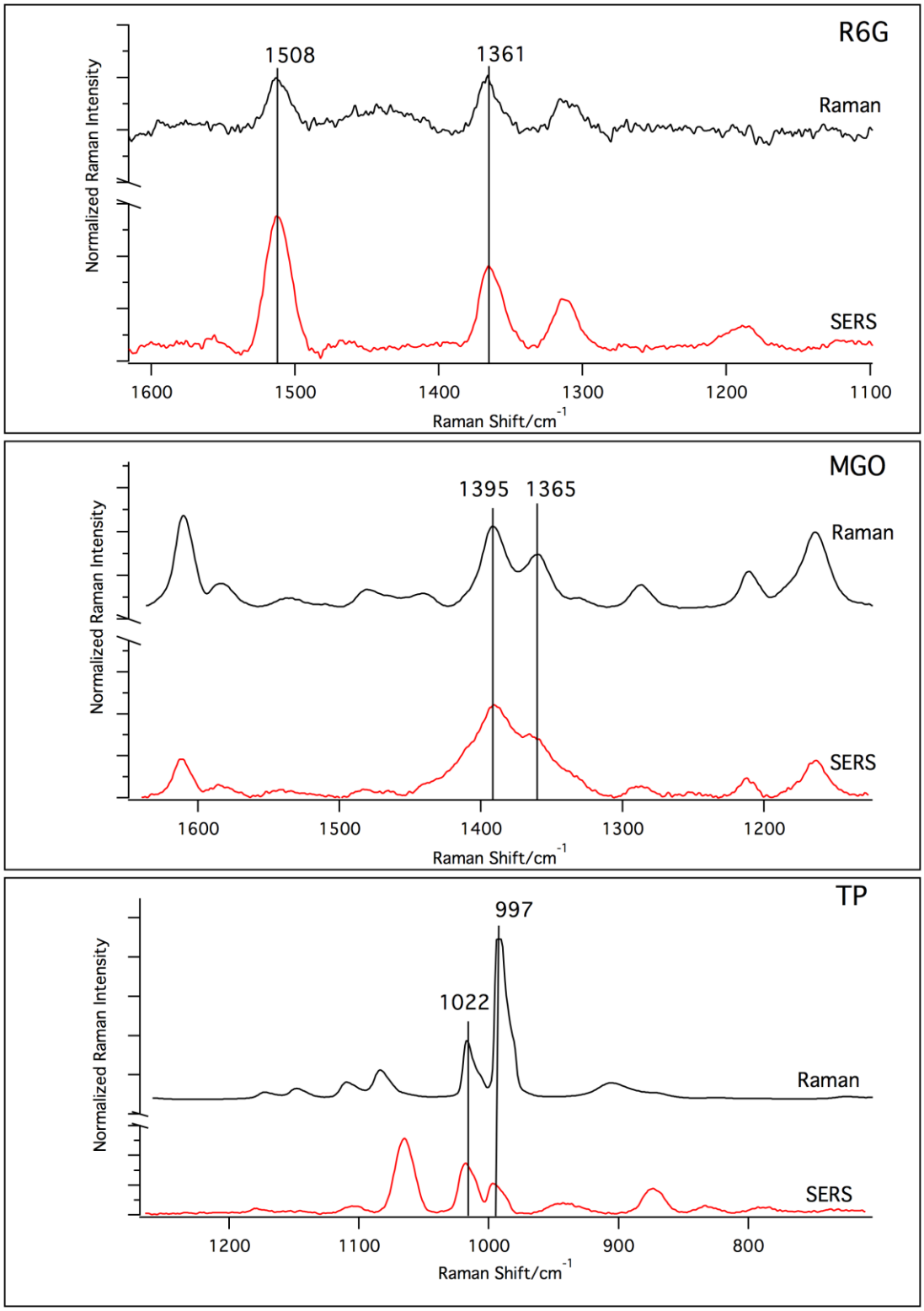

Figure 4. Offset Raman and SERS spectra of R6G, MGO and TP (baseline corrected). 65 nm AgNPs were used as the SERS substrate. Alaser excitation of 785 nm was used with a 20 second exposure time and 5 accumulations.